Laser Scanning for Modeling Spatial Area: Theory and Technology

M.S. Hany[1], Z.Z. El-shiekha[2] and F.H. Zarzoura[3]

[1] Civil engineering Department, Delta Higher Institute of Engineering and Technology in Mansoura, Egypt-email: monasalah1631993@gmail.com

[2] Public Works Engineering Department, Mansoura university, Mansoura, Egypt-email: zmze283@mans.edu.eg

[3] Public Works Engineering Department, Mansoura university, Mansoura, Egypt-email: fawzihamed@mans.edu.eg

Corresponding Author: Mona Salah

Abstract: **At the present time, laser scanning technology has become one of the most widely used technologies, and its importance appears in various fields and is not limited to one field. It also gets support from satellites and obtains an analysis of the area to be scanned, with the help of geographic information. This depends on the use of the Geographic Information System (GIS) program. GIS), thus enabling urban spatial planning, infrastructure design, and object monitoring and control. One of the types of laser scanning is the terrestrial laser scanning system. Therefore, it is necessary to study this technology in terms of the principles on which it depends in measurement, the type of laser beams used in the scanning process, which works to obtain the required accuracy and details, clarifying errors that affect the accuracy of the scanned data and working to avoid them, studying mathematical models, working to make all individual scanned data in one coordinate system, calibrating spherical reservoirs and working on developing them when scanning using a scanner Laser scanning, calibration of digital cameras and work to increase their speed and accuracy by using the ground scanner.**

Keywords-Terrestrial Laser Scanning (TLS), Mathematical model, Individual sources of errors, The imaging processing theory, The calibration of ball tanks, non-metric digital camera calibration technology.

I. INTRODUCTION

There is always a need for surveying, and it has a clear importance since the beginning of civilization. But in previous eras, some traditional methods of surveying were used, and they had many obstacles that appear in front of the user, and the inability to use them in all applications, for this, a new method for obtaining data was detected and applied, which is the use of the laser scanning system **[1]**. There are more than one type of laser scanner: airborne laser scanning (ALS), ground laser scanning (TLS), and micro-laser scanning (Micro-LS). All of these types depend on two types of capture systems, including: laser and radar. It is distinguished by coherence of radiation and beam spacing, thus increasing accuracy, which gives better details compared to other imaging systems **[2]**.

Systematic studies are used that seek the technological and theoretical development of the laser scanner to create three-dimensional geographic information models, analyze the laser scanner data, work on simulating the area, and increase the accuracy of the survey, including: (the accuracy of the height of the ground scanner, matching the details of the three-dimensional models with data values), recording and studying the principles of measurement used, and the development and treatment of photographic measurement theory, all this to control the accuracy of the results to suit the requirements of the work **[3]**.

II. METHODOLOGY

a. Laser scanning technology:

The laser scanning technology, especially the laser ground scanning system, can obtain millions of 3D points with very high accuracy, and the time taken is short, and there is more than one position to operate the scanners: the fixed or portable position. There are some programs that depend on the operation and all of them refer to the georeferenced (X, Y, Z) to a local or global reference network **[4]**.

b. Scanning principles for laser scanners:

Scanners are designed according to three scanning principles **[2]**:

- Pulse-based scanners: It is considered one of the most widely used principles in which the device sends a signal in the direction of the object to be scanned and receives the reflected signal, and thus the time (t) that it took to travel back and forth is measured by the detector and by knowing the speed of the signal that represents the speed of light, which is (c) = 299,792,458 m / s. The distance (d) from the device to the surface of the object is calculated from equation (1) **[1]**.

$$D = (c * t)/2 \qquad (1)$$

- Phase-based scanners: The device transmits a signal consisting of a continuous wave (c/w) and receives the reflected signal. Knowing the phase difference between the transmitted and received wave (Δφ) and calculating the wavelength of the signal (λ), given that (n) is an unknown

number of wavelengths between the device and the object, the distance (D) from the equation is calculated (2) **[5]**.

$$D = (\Delta\varphi/2\pi) * (\lambda/2) + \big((\lambda/2)\big) * n \qquad (2)$$

-Optical triangulation method, where the transmitter sends a laser beam at the surface of the object and the CCD

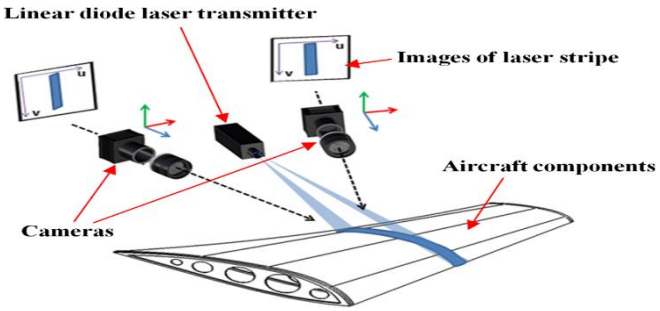

camera detects the laser beam at the other end of the base. The 3D coordinates of the laser beam on the surface of the object are derived from the resulting triangle. Two CDD cameras are used, one at the end of the base and called a dual camera solution, to improve resolution as shown in Figure 1. It is suitable for precision surveying such as sculpture in cultural heritage documentation **[6]**.

Fig 1: Triangulation laser scanning principle [6].

c. Characteristics of the laser beam:

It is necessary to know the propagation characteristics of a laser beam. Most of the beams used as a source for the laser beam are Guess beams, and they are distinguished by their shape and expected smooth and easy development. During propagation, some diffraction appears in space, as shown in the figure (2). Given both the wavelength (λ) and the radius of the laser beam at the waist ($\omega_\circ$), the beam spacing of the laser beam at the waist ($\gamma_\circ$) is calculated from equation (3) **[7]**.

$$\gamma_\circ = \lambda/(\pi * \omega_\circ) \qquad (3)$$

Knowing all the previous characteristics of the laser beam, the radius of the laser beam is calculated as a function of the distance (Z) from equation (4) **[7]**.

$$\omega\,(z) = \sqrt{1 + (\lambda z/\pi * {\omega_\circ}^2)^2} \qquad (4)$$

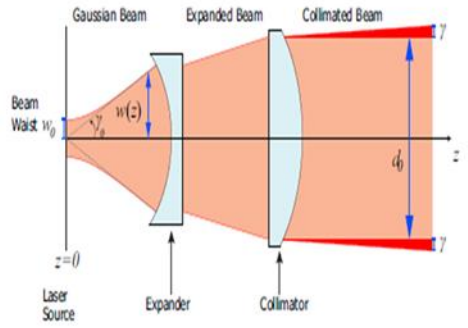

Figure .2. The propagation of the Gaussian beam of the laser beam [7].

d. Imprint of the laser beam on the object:

The radius of the laser beam is directly proportional to the distance, scanners aim to obtain a small imprint on the surface of the object to allow the best scanning results. There are two types of fingerprints, As shown in the figure (3) **[1]**:

- The fall of a perpendicular beam on a flat surface, ($d_\circ$) is the diameter of the beam after passing through the beam collecting lenses in the device, therefore the effect of the Imprint is calculated from equation (5).

$$d\,(z) = d_\circ + 2z\,tan\,\gamma \qquad (5)$$

The incident of the ray on an inclined surface, results in a major axis (dM (z)) and a minor axis (dm (z)), where (α) is the incidence of the laser beam and the distance of the plane surface to the origin (z). The Imprint axes are calculated from equation (6).

$$dM(z) = d_\circ + 2z(\sin(2\gamma)/(\cos(2\alpha)) + \cos(2\gamma))) \qquad (6)$$

$$dm(z) = d_\circ + 2z\big(\sin(2\gamma)/\big(\cos(\alpha) + (1 + \cos(2\gamma))\big)\big)$$

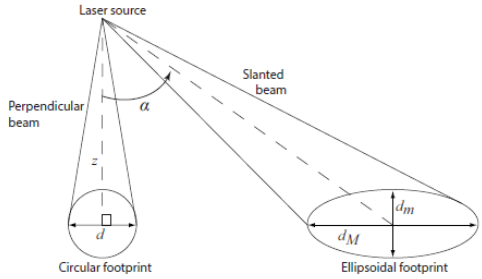

Figure.3. The fingerprint on the surface of the object [1].

e. Data acquisition procedure:

In the foreground is setting reference points, choosing the best location and the most suitable height for the device to ensure maximum coverage and help in combining reconnaissance scenes, putting the results into a single coordinate system to remove the consequences. After that comes the process of processing and using formatting software, then finally recording and archiving the data **[8]**.

f. Errors affecting the accuracy of results:

The accuracy of the results is affected by many factors, including: the error in the scanner, as it contains errors in the axes, part of the error can be removed, thus increasing the measurement accuracy by 40%, the mixed edge error occurs when the laser beam falls on two adjacent surfaces and the reflected signal of the two surfaces merges together. Error resulting from laser beam divergence due to distance traveled and given range related to beam waist location (ρ_w), beam

radius (w), and minimum beam radius (w_o). The beam spacing is calculated from equation (7) **[9]**.

$$\omega_{(\rho\omega)} = \sqrt{1 + (\lambda\rho\omega/\pi\omega_{\circ}^{2})^{2}} \quad (7)$$

Errors in a rangefinder. For a pulse-based scanner, the rangefinder depends on knowing the time of pulse transmission (T_{Rep}), taking into account the signal noise ratio (SNR), and the speed of light (c), compute the range accuracy from equation (8), To calculate the accuracy of the phase-based scanner range by measuring the modified wavelength difference (λm) and signal noise ratio (SNR), equation (9) is used **[9]**.

$$\delta_{r} \approx (c\, T_{Re\,P})/\left(2\sqrt{SNR}\right) \quad (8)$$

$$\delta_{r} \approx \lambda m/4\pi\sqrt{SNR} \quad (9)$$

Errors resulting from external conditions, temperature, as there is no device that works properly except at certain temperatures, and the laser beam that is exposed to refraction during propagation through the air, and both errors affect the measurements of distances and angles. Experimental studies have shown that errors due to refraction are sinusoidal in nature, and thus the correction values for angular measurements vary with time. Since the measurement time at a station ranges from 1.5 to 2 hours, the angle measurement correction value must be determined as a function of time **[10]**.

The error resulting from the metrological characteristics of the surveyed objects, and this error affects the distance measurement only. One source of this error is the reflection given the incident light intensity (I(λ)), the diffuse reflection coefficient ($k_d(\lambda)$), the angle of the incident light, and the normal vector of the incident light. Surface (θ), the reflectance coefficient of the scanned surface is calculated from equation (10), the color of the scanned object also greatly affects the scattered signal and it is clear from the simulation results that the distance measurement error caused by the metrological characteristics of the objects mostly ranges from 1 to 3 cm. Errors due to the difference in color or reflectance in objects can be reduced by calibrating the scattered signal based on the combined processing of the scanner measurement results and information about the color of the object obtained by photography**[11]**.

$$I\text{reflected}(\lambda) = I_{i}(\lambda) * k_{d}(\lambda) * \cos\theta \quad (10)$$

The theory and technology of the laser scanner seek to obtain high accuracy of the measurements and this can be done by knowing the mean square error generated by the input function to measure the distances ($m_{F(t)}^{2}$) and the variation of the horizontal and vertical angles of the distance due to vibration ($m_{Rvibration}$, $m_{\varphi vibration}$,and $m_{\theta Vibrate}$) and a distance error Individual measurement, horizontal and vertical angles obtained from the measuring instrument scan results ($m_{Rmetrol}$, $m_{\varphi metrol}$,and $m_{\theta metrol}$) and the value of systematic mechanical errors ($m_{\sigma R}$, $m_{\sigma\varphi}$,and $m_{\sigma\theta}$). Thus, the mean squared error of standard distances and horizontal and vertical angles is expressed from equation (11), where absolute humidity (E), temperature (T), and atmospheric pressure (P) **[10]**.

$$m_{R} = \sqrt{m_{F(t)}^{2} + m_{R(T,P,E)}^{2} + m_{R\,vibrate}^{2} + \left(\left(m_{Rmetrol}^{2} - m_{\delta R}^{2}\right)/\sqrt{n}\right)} + m_{\delta R}^{2}$$

$$m_{\varphi} = \sqrt{m_{\delta\varphi(T,P,E)}^{2} + m_{\varphi\,vibrate}^{2} + \left(\left(m_{\varphi metrol}^{2} - m_{\delta\varphi}^{2}\right)/\sqrt{n}\right)} + m_{\delta\varphi}^{2}$$

$$m_{\theta} = \sqrt{m_{\delta\theta(T,P,E)}^{2} + m_{\theta\,vibrate}^{2} + \left(\left(m_{\theta metrol}^{2} - m_{\delta\theta}^{2}\right)/\sqrt{n}\right)} + m_{\delta\theta}^{2} \quad (11)$$

g. Coordinate system of laser scanner measurements:

It is necessary to make all the points captured by the scanner into one specific coordinate system, knowing (X, Y, and Z) coordinates of the scanning points of the scanner coordinate system and (X_0, Y_0,and Z_0) coordinates that are checked by the (Oxyz) system, The coordinates of points from one system to another can be converted from equation (12), taking into account (a_1, a_2 ... c_3), which is the cosine direction, which is a function of the angles ε, η, ξ, and the cosine of the orientation system coordinate matrix**[12]**.

$$\begin{bmatrix} X_{BH} \\ Y_{BH} \\ Z_{BH} \end{bmatrix} = \begin{bmatrix} X_{\circ} \\ Y_{\circ} \\ Z_{\circ} \end{bmatrix} + A \begin{bmatrix} X \\ Y \\ Z \end{bmatrix} \quad (12)$$

Where:

$$A = \begin{bmatrix} a_1 & a_2 & a_3 \\ b_1 & b_2 & b_3 \\ c_1 & c_2 & c_3 \end{bmatrix}$$

To calculate the coefficients (X 0, Y 0, Z 0, ε, η,and ξ) there are two ways:

- Calculation method (X 0, Y 0) by placing the device above the reference points with known coordinates, (Z0) is determined by the height of the device. But these measurements have an error rate, considering that the outward direction of the angle scan is therefore very small (cos ε ≈ cos η ≈ 1, sin ≈ and sin). The square error of ($m_{Y_{BH}}$ $m_{Z_{BH}}$, $m_{X_{BH}}$) is expressed from equation (13) **[13]** .

$$m_{X_{BH}}^{2} = m_{X_O}^{2} + m_{\xi}^{2} \cdot Y^{2} + m_{\varepsilon}^{2} \cdot Z^{2}$$
$$m_{Y_{BH}}^{2} = m_{Y_O}^{2} + m_{\xi}^{2} \cdot X^{2} + m_{\eta}^{2} \cdot Z^{2} \quad (13)$$
$$m_{Z_{BH}}^{2} = m_{Z_O}^{2} + m_{\varepsilon}^{2} \cdot X^{2} + m_{\eta}^{2} \cdot Y^{2}$$

- The analytical method, which reflects the error found during the least squares solution of the equations, depends on the layout geometry and the number of special stamps.

Therefore, to move from the scanning coordinate system to the external system, equation (14) is used, taking into account that the values measured by the laser land survey are (R, φ, and θ). If the special stamps used are three stamps or more, the measurement weights are taken into account and expressed It is obtained from Equation (15), which is used to calculate the corrections for (δX_0, δY_0, δZ_0, δ ε, δη,and δξ) that are corrected after completing the iterative process. Measurements must be made equally with each other when using the method of least squares in the equations to solve the outward orientation problem **[14]**.

$$\begin{aligned} 1^{'} &= X_0 + a_1 R\cos\varphi\sin\theta + a_2 R\sin\varphi\sin\theta + a_3 R\cos\theta \\ &\quad - X_{BH} = 0 \\ 2^{'} &= Y_0 + b_1 R\cos\varphi\sin\theta + b_2 R\sin\varphi\sin\theta + b_3 R\cos\theta \\ &\quad - Y_{BH} = 0 \\ 3^{'} &= Z_0 + c_1 R\cos\varphi\sin\theta + c_2 R\sin\varphi\sin\theta + c_3 R\cos\theta \\ &\quad - Z_{BH} = 0 \end{aligned} \tag{14}$$

$$\begin{bmatrix} N_1 & N_2 \\ N_2^T & N_3 \end{bmatrix} \cdot \begin{bmatrix} \delta X_0 \\ \delta Y_0 \\ \delta Z_0 \\ \delta\varepsilon \\ \delta\eta \\ \delta\xi \end{bmatrix} + \begin{bmatrix} \sum_{i=1}^{n} P_{x_i} \lfloor X_i \\ \sum_{i=1}^{n} P_{y_i} \lfloor Y_i \\ \sum_{i=1}^{n} P_{z_i} \lfloor Z_i \\ \sum_{i=1}^{n} P_{X_i} \frac{\partial F_1}{\partial \varepsilon} \lfloor_{X_i} + \sum_{i=1}^{n} P_{Z_i} \frac{\partial F_3}{\partial \eta} \lfloor Z_i \\ \sum_{i=1}^{n} P_{X_i} \frac{\partial F_1}{\partial \eta} \lfloor_{X_i} + \sum_{i=1}^{n} P_{Y_i} \frac{\partial F_2}{\partial \eta} \lfloor_{Y_i} + \sum_{i=1}^{n} P_{Z_i} \frac{\partial F_3}{\partial \eta} \lfloor Z_i \\ \sum_{i=1}^{n} P_{X_i} \frac{\partial F_1}{\partial \xi} \lfloor_{X_i} + \sum_{i=1}^{n} P_{Y_i} \frac{\partial F_2}{\partial \xi} \lfloor_{Y_i} + \sum_{i=1}^{n} P_{Z_i} \frac{\partial F_3}{\partial \xi} \lfloor Z_i \end{bmatrix} \tag{15}$$

Calculate the linear standard deviation of the orientation direction X0 using equation (16). Similarly, the standard deviations of the other elements are determined using equation (17), given that ($\Delta\,(ATPA)^{-1}$) is the determinant of the matrix and ($\Delta X_0 X_0$, $\Delta X_0 Y_0$, ..., $\Delta\xi\xi$) are algebraic complements of the corresponding element, and taking into account that the external angle of the scan is small (that cos ε ≈ cos η ≈ cos ξ 1, sin ε, sin η ≈ η and sin ≈ ξ), the signs Those located at the same distance from the scanner and are similar to the plane parallel to XY. Therefore, the diagonal elements of the matrix are calculated by equation (18) by knowing the number of signs (n) .The remaining elements outside the diagonal of the matrix are derived from equation (19), The rest of the elements of the matrix Q are equal to zero (19)**[14]**.

$$m_{X_0} = \mu\sqrt{Q_{X_0X_0}} \tag{16}$$

Where:

$$\mu = \sqrt{\frac{\sum_{i=1}^{3n} PV_i^2}{3n-6}}$$

$$(A^TPA)^{-1} = Q = \frac{1}{\Delta A^TPA}\begin{bmatrix} \Delta X_0X_0 & \Delta X_0Y_0 & \Delta X_0Z_0 & \Delta X_0\varepsilon & \Delta X_0\eta & \Delta X_0\xi \\ \Delta X_0Y_0 & \Delta Y_0Y_0 & \Delta Y_0Z_0 & \Delta Y_0\varepsilon & \Delta Y_0\eta & \Delta Y_0\xi \\ \Delta X_0Z_0 & \Delta Y_0Z_0 & \Delta Z_0Z_0 & \Delta Z_0\varepsilon & \Delta Z_0\eta & \Delta Z_0\xi \\ \Delta X_0\varepsilon & \Delta Y_0\varepsilon & \Delta Z_0\varepsilon & \Delta_{\varepsilon\varepsilon} & \Delta_{\varepsilon\eta} & \Delta_{\varepsilon\xi} \\ \Delta X_0\eta & \Delta Y_0\eta & \Delta Z_0\eta & \Delta_{\varepsilon\eta} & \Delta_{\eta\eta} & \Delta_{\eta\xi} \\ \Delta X_0\xi & \Delta Y_0\xi & \Delta Z_0\xi & \Delta_{\varepsilon\xi} & \Delta_{\eta\xi} & \Delta_{\xi\xi} \end{bmatrix} \tag{17}$$

$$\left\{\begin{array}{c} Q_{X_0X_0} = Q_{Y_0Y_0} = \frac{1+\cos\theta^2}{n\sin\theta^2} \\ Q_{Z_0Z_0} = \frac{1}{n} \\ Q_{\varepsilon\varepsilon} = Q_{\eta\eta} = \frac{2}{nR^2\sin\theta^2} \\ Q_{\xi\xi} = \frac{1}{nR^2\sin\theta^2} \end{array}\right\} \tag{18}$$

$$Q_{X_0\varepsilon} = Q_{Y_0\eta} = -\frac{2\cos\theta}{nR\sin\theta^2} \tag{19}$$

Experimental laser land survey studies have shown that the values of the vertical directions are from 76 to 85, and the distance R is from 10 to 30 meters. Also, it is impossible to guarantee that special signs will be visible within a hundred meters, especially if the laser ground survey is carried out in very crowded areas, Thus, it is difficult to achieve accuracy in determining the angular elements of the outer direction of the survey using the analytical method only, to get a better definition of the outward orientation of the survey, the two methods should be combined **[13]**.

h. Generate 3D models according to the scanner data:

The error in the spatial location of the scanner station and for calculating the accuracy of the scanner spatial location (AOSP) is derived from equation (20), and the error value in the spatial direction of the scanner location can be calculated by equation (21) **[15]**.

$$AOSP = \sqrt{Q_{X_0X_0} + Q_{Y_0Y_0} + Q_{Z_0Z_0}} \tag{20}$$

$$AOSO = \sqrt{Q_{\varepsilon\varepsilon} + Q_{\eta\eta} + Q_{\xi\xi}} \tag{21}$$

There are two ways to create 3D models according to the scanner data, namely: surfaces, and geometric objects. Knowing both the error caused by the external orientation of

the scans (m_{OR}) and the error in determining the coordinates of the model points caused by the influence of errors in the scanner tool, the external environment and the metrological properties of the object being scanned. Cleared out (m_{ISR}) computes the error in the model based on the surfaces from equation (22) **[16]**.

$$m_K^2 = m_{OR}^2 + m_{ISR}^2 \qquad (22)$$

Studies have shown that the error in creating 3D models using surfaces ranges between (1:7) m. As for the error of using geometric objects, the accuracy of the 3D models depends on several factors, including: random deviations from the mathematical model, the unique measurements of the ground laser scanner and its accuracy, and subjective errors when using the semi-automatic mode **[15]**.

Evaluate the accuracy of creating 3D models using geometric objects by knowing the coefficient whose value depends on the chosen position of the structure of the 3D model (K), the value (k) is obtained if the scanning mode is automatic (k = (0.95-1.0)), and in the semi-mode automatic (k = (0.70-0.85)) and interactive mode (k = (0.30-0.70)). Equations (23 and 24) are used according to the laser beam spacing (Ψ) **[6]**.

- for scanners with Ψ> 1 m $m_L = 0.01610 * k * \Psi$ (23)

- for scanners with Ψ < 1 m. $m_L = 0.12499 * k * \Psi$ (24)

i. Photographic measurement:

Photogrammetry is used to process laser ground scanning data, converting the laser scanning data into a set of virtual images of the corresponding central projection. Because the coordinates of the image display center (x_0, y_0) are equal to zero and the spatial coordinates of the body points (X_M, Y_M, Z_M), equation (25) is used to relate the coordinates of the image points to the spatial coordinates of the corresponding points, which is a linear relationship. To obtain the measured distance, a linear relationship is used. Equation (26) and express them as follows **[7]**.

$$y_{i,j} - y_0 = f[(e_2(X_M - X_0) + g_2(Y_M - Y_0) + q_2(Z_M - Z_0))/(e_1(X_M - X_0) + g_1(Y_M - Y_0) + q_1(Z_M - Z_0))] \qquad (25)$$

$$z_{i,j} - z_0 = f[(e_3(X_M - X_0) + g_3(Y_M - Y_0) + q_3(Z_M - Z_0))/(e_1(X_M - X_0) + g_1(Y_M - Y_0) + q_1(Z_M - Z_0))]$$

$$R = \sqrt{(X_M - X_0)^2 + (Y_M - Y_0)^2 + (Z_M - Z_0)^2} \qquad (26)$$

The camera can be placed inside the scanner or outside the scanner as it can be installed on the rotating head of the scanner, so the digital images and the virtual image become identical beam and the same focal length. By knowing the accuracy of the horizontal and vertical angle of scanning (Δφ, Δθ) and the values of horizontal and vertical angles measured from the optical axis of the virtual image (φ, θ), distortions are removed using equation (27) **[17]**.

$$\delta_{panoramic\ horizontal} = 2f\left[\left(tg(\Delta\varphi/2)\right)/\left(\cos\varphi^2 - (\sin\varphi^2)\cdot tg^2(\Delta\varphi/2)\right)\right]$$
$$\delta_{panoramic\ vertical} = 2f\left[tg(\Delta\theta/2)/\left(\cos\varphi^2 - (\sin\varphi^2)\cdot tg^2(\Delta\varphi/2)\right)\right] \qquad (27)$$

Image calibration is done after the initial processing of the scans by knowing the values of the image element size on the ground (δ), the element size of the CCD matrix ($d_{x,y}$), the focal length of the digital camera (f), and the coefficient of perception of the smallest object size in the image (k). Equation (28) expresses the calculation of the distance R from the digital camera installed on the scanner to an object with specific details, knowing the size of the CCD matrix (l_x, l_y), the horizontal and vertical angles of the digital camera's field of view can be calculated from equation (29), to calculate the area using the equation (30) given both the longitudinal overlap of images (p) and the transverse overlap of images (q), the number of images required to cover the survey. calibration is done after the initial processing of the scans by knowing the values of the image element size on the ground (δ), the element size of the CCD matrix (dx, y), the focal length of the digital camera (f), and the coefficient of perception of the smallest object size in the image (k). Equation (28) expresses the calculation of the distance R from the digital camera installed on the scanner to an object with specific details, knowing the size of the CCD matrix (lx, ly), the horizontal and vertical angles of the digital camera's field of view can be calculated from equation (29), to calculate the area using the equation (30) given both the longitudinal overlap of images (p) and the transverse overlap of images (q), the number of images required to cover the survey**[17]**.

$$R = \delta f / k d_{x,y} \qquad (28)$$

$$\varphi_{ck} = 2arctg\left(l_x d_{x,y}/2f\right) \qquad (29)$$

$$\theta_{ck} = 2arctg\left(l_y d_{x,y}/2f\right)$$
$$n_x = (\varphi_{ck}/\varphi_{ck}(100 - q)) * 100\% + 2$$
$$n_y = (\theta_{ck}/\theta_{ck}(100 - q)) * 100\% + 2 \qquad (30)$$

j. Procedure for the calibration of ball tanks:

In the first stage to determine the main capacity of the tank, the basic height of the tank must be determined, and it is measured at least twice while the tank is empty. To take into account the measurements, the discrepancy between the results of the two measurements should not exceed 2 mm. Then the arithmetic mean of the two measurements is taken to determine the height of the base of the tank (Hb). The best locations for placing at least two surveying devices are determined, taking into account the internal structures of the tank. Then, the results of measurements (pressure and temperature) of both the

environment and the internal space of the tank are entered into a specialized computer to control the scanner. When scanning with two or more scanner stations, in which special marks are installed in the internal space of the tank (at least four) so that they do not block the internal structures and the surface of the tank and are visible from all sides. Their type and size depend on the applicable scanner model. Tank capacity is determined using NLS Rapid Form and Cyclone software and software developed by FSBEI HPE "SGGA" and embedded in AutoCAD software **[18]**.

-In the first stage, the relative orientation of the surveys is carried out, and then the data obtained during the survey are exported to the Rapid Form program used to create 3D models of objects in the form of a grid surface of the inner walls of the tank,(The maximum polygons should not exceed 5 cm). Then filter the set of points from the false measurements that occur when the signals are reflected back.

- The next step in the Cyclone program is to combine the two models obtained. According to the general model obtained for the inner walls and structures of the tank, the height of the tank structure is determined from equation (31):

$$H_{tank} = Z_{max} - Z_{min} \qquad (31)$$

Where:

H_{tank}: the height of the tank;

Z_{max} and Z_{min}: the maximum and minimum marks of the tank, As shown in Figure (4).

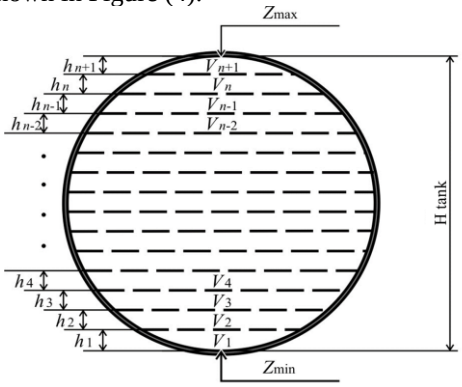

Figure .4. Tank model [18].

- Then, the Rapid Form program is used to dissect the 3D model of the tank by horizontal levels with a distance of 1 cm for the number of layers, and the dissection starts from the bottom. Then the corresponding spherical layer volume is calculated for each level, is carried out using the program developed by the FGBOU VPO "SGGA" in the AutoCAD software package, From the equation (32), (33), (34) **[19]**:

$$U_1^{s.tank} = \pi.((H_{tank}/2).h_1^2 - (h_1^3/3)) \qquad (32)$$

$$U_j^{s.tank} = \left(\left(S_{j-1} + S_j\right).h/2\right) + (\pi.\mathrm{h}^3/6) \qquad (33)$$

$$U_{n+1}^{s.tank} = \pi((H_{tank}/2).h_{n+1}^2 - (h_{n+1}^3/3)) \qquad (34)$$

Where:

h 1: height of the first spherical layer equal to 0.01 m.

j: the number of spherical layers, which varies from 2 to n (determined by rounding down to an integer value).

h: height of each(j) the spherical layer equal to 0.01 m (1 cm).

hn + 1: height (n + 1) the spherical layer, it is calculated from the equation (35):

$$h_{n+1} = H_{tank} - (h_1 + h.(n-1)) \qquad (35)$$

-Then the capacity of the tank is determined and calculated without taking into account the $U^{s.tank}$ structures. From Equation (36), as for the volume of the spherical layer (g) corresponding to the level (g) cm, taking into account the structure, it is calculated from Equation (37), so the U^{tank} tank capacity is calculated using Equation (38):

$$U^{s.tank} = U_1^{s.tank} + \sum_{j=2}^{n} U_j^{s.tank} + U_{n+1}^{s.tank} \qquad (36)$$

$$\mathrm{U_g^{tank}} = \mathrm{U_g^{s.tank}} - \mathrm{U_g^{const}} \qquad (37)$$

$$\mathrm{U^{tank}} = \sum_{g=1}^{n+1} \mathrm{U_g^{tank}} \qquad (38)$$

Where:

$U_g^{s.tank}$: volume g- th spherical layer, determined by formula (5.35) for g = 1, according to formula (5.36) for g = j (from 2 to n) and by formula (5.37) for g = (n + 1);

U_g^{const}: the volume of internal structures for each g-the spherical layer calculated by Rapid Form software.

The relative error in calculating the tank capacity is determined using the developed Sphere Rezer program in accordance with RMG 62, From the equation (39):

$$\delta = k.\sqrt{\delta_U^2 + \delta_{mod}^2 + \delta_{deduction}^2} \qquad (39)$$

Where:

k: coefficient equal to 1.1.

δ_U, δ_{mod}, $\delta_{deduction}$: the components of the relative calculation error in tank capacities, determined by the equation (40):

$$\delta_U = max\left(\delta_{U_g}\right)$$

$$\delta_{maud} = max\left(\delta_{maud_g}\right) \qquad (40)$$

$$\delta_{deduction} = max\left(\delta_{daduction_g}\right)$$

Where:

δ_{maud_g} : relative simulation error;

$\delta_{daduction_g}$: relative error;

δ_{U_g}: relative error in calculating the volume, it is concerned with all spherical classes, determined from the equation (41):

$$\delta_{U_g} = \left(\left|\Delta U_g\right|/U_g^{s.tank}\right)100\% \qquad (41)$$

Where:

ΔU_g: the absolute error in calculating the volume, determined in accordance with MI 2083, It is calculated from the equation (42):

$$\Delta U_g = k.\sqrt{\sum_{i=1}^{m}\left(\partial U_g/\partial x_i\right)^2.\Delta x_i^2} \qquad (42)$$

Where:

K: a correction factor equal to 1.1.

Ug: volume function depending on the input quantities xi.

Δ xi: the absolute error of measurements of the values obtained as a result those of direct measurements.

To determine the absolute error in the calculation of the volume of the first spherical layer, the partial derivatives of the volume function must be calculated from the equation (43):

$$\partial U_1^{s.tank}/\partial H_{tank} = \pi.h_1^2/2$$
$$\partial U_1^{s.tank}/\partial h_1 = \pi.H_{tank}.h_1 - \pi.h_1^2 \qquad (43)$$

Where:

H_{tank}: the height of the tank, calculated by the equation (31);

h_1: the height of the first spherical layer, equal to 0.01 m.

Absolute volume measurement error Δ U1 The first spherical layer is calculated using the expressions (41) and (42) and expressed from the equation (44):

$$\Delta U_1 = \sqrt{(\pi^2.h_1^4/4).\Delta H_{tank}^2 + (\pi.H_{tank}.h_1 - \pi.h_1^2)^2.\Delta h_1^2} \qquad (44)$$

Where:

ΔH_{tank}, Δh_1: absolute errors of measurements of the tank height and spherical layer, equal to the distance measurement errors Δ R, determined by the equation (45):

$$\Delta R = S_R.t \qquad (45)$$

Where:

S_R = 0.004 m (4 mm), limits of the permissible standard deviation of distance measurements.

t: Student's coefficient equal to 2.776 for the confidence level P = 95% and the number of observation results n = 5.

Using expressions (41) and (42), to determine the relative measurement error of δU_1 the first spherical layer, the equation (46) is used, the relative error in the calculation of the volume of the ball layer $\delta_{U_{(n+1)}}$ is calculated by the equation (47):

$$\delta U_1 = (100\%/U_1^{s.tank}).k.\pi.\Delta R.\sqrt{1.25.h_1^4 + H_{tank}.h_1^2(H_{tank} - 2.h_1)} \qquad (46)$$

Where:

$U_1^{s.tank}$: the volume of the first spherical layer, From the equation (32).

$$\delta_{U_{(n+1)}} = \left(100\%/U_1^{s.tank}\right).k.\pi.\Delta R.\sqrt{1.25h_{n+1}^4 + H_{tank}.h_{n+1}^2.(H_{tank} - 2h_{n+1})} \qquad (47)$$

Where:

$U_1^{s.tank}$: the volume of the last spherical layer, calculated by the equation (32);

h_{n+1}: height (n + 1) of the spherical layer.

To determine the relative error in calculating the size of the spherical layer (j), the values of the cross-sectional area must be expressed through the distances R_{j-1} and R_j and the angles θ_{j-1} and θ_j. For the measurements of the scanner, the equation (48) is used, the relative error in calculating the volume (j) of the first spherical layer, the partial derivatives of the volume function are calculated by the equation (49):

$$U_j^{s.tank} = \left(\left(S_{j-1} + S_j\right).h/2\right) + (\pi.h^3/6) =$$
$$(\pi.b^2.h + \pi.a^2.h/2) + (\pi.h^3/6) =$$
$$\left(\pi.R_{j-1}^2.\sin(\theta_{j-1})^2.h/2\right) + \left(\pi.R_j^2.\sin(\theta_j)^2.h/2\right) + (\pi.h^3/6) \qquad (48)$$

Where:

$U_j^{s.tank}$: The volume of the spherical layer (j), calculated with the formula (33).

j: serial number of the spherical layer (varies from 2 to n).

h: The height of the spherical layer (j) is equal to 0.01 m.

$$\left(\partial U_j^{s.tank}/\partial R_{j-1}\right) = \pi.h.R_{j-1}.\sin(\theta_{j-1})^2$$
$$\left(\partial U_j^{s.tank}/\partial R_j\right) = \pi.h.R_j.sin(\theta_j)^2$$
$$\left(\partial U_j^{s.tank}/\partial \theta_{j-1}\right) = \pi.h.R_{j-1}^2.\sin\left(\theta_{j-1}\right).\cos(\theta_{j-1}) \qquad (49)$$
$$\left(\partial U_j^{s.tank}/\partial \theta_j\right) = \pi.h.R_j^2.sin\left(\theta_j\right).cos(\theta_j)$$
$$\left(\partial U_j^{s.tank}/\partial h\right) = \left(\pi.R_{j-1}^2.\sin(\theta_{j-1})^2/2\right) + \left(\pi.R_j^2.\sin(\theta_j)^2/2\right)$$

The absolute volume error ΔUj for the spherical layer is calculated using the equation (50):

$$\Delta U_j = k.\sqrt{\Lambda_1 + \Lambda_2 + \Lambda_3 + \Lambda_4 + \Lambda_5}$$
$$\Lambda_1 = \pi^2.h^2.R_{j-1}^2.\sin(\theta_{j-1})^4.\Delta R_{j-1}$$
$$\Lambda_2 = \pi^2.h^2.R_j^2.sin(\theta_j)^4.\Delta R_j$$
$$\Lambda_3 = \pi^2.h^2.R_{j-1}^4.\sin(\theta_{j-1})^2.\cos\left(\theta_{j-1}\right)^2.\Delta\theta_{j-1}^2 \qquad (50)$$
$$\Lambda_4 = \pi^2.h^2.R_j^4.sin(\theta_j)^2.cos\left(\theta_j\right)^2.\Delta\theta_j^2$$
$$\Lambda_5 = (1/4).\left(\pi.R_{j-1}^2.\sin\left(\theta_{j-1}\right)^2 + \pi.R_j^2.\sin\left(\theta_j\right)^2 + \pi.h^2\right)^2.\Delta h^2$$

Where:

ΔR_{j-1}, ΔR_j, Δ h: absolute errors of distance and height measurements spherical layer, equal to the distance measurement errors Δ R(m), determined by the formula (45).

$\Delta\theta_{j-1}$, $\Delta\theta_j$: absolute measurement errors of vertical angles, equal to angular measurement errors Δθ(rad) determined by the equation (51):

$$\Delta\theta = S_\theta.t \qquad (51)$$

Where:

Sθ: the limits of the permissible standard deviation of measurements of angles= 5.82 10- five rad (12 ");

t: Student's coefficient equal to 2.571 for the confidence level, P = 95% and the number of observation results n = 6.

The relative error of the volume measurements of the spherical layer δU_j is determined, from the equation (52):

$$\delta U_j = \left(100\%/U_j^{s.tank}\right).k.\pi\sqrt{\Phi_1 + \Phi_2 + \Delta R^2.[\Phi_3 + \Phi_4]}$$

$$\Phi_1 = \Delta\theta^2.h^2.\left(R_{j-1}^4.\sin\left(\theta_{j-1}\right)^2.\cos\left(\theta_{j-1}\right)^2\right)$$

$$\Phi_2 = R_j^4.\sin\left(\theta_j\right)^2.\cos\left(\theta_j\right)^2 \quad (52)$$

$$\Phi_3 = R_{j-1}^2.\sin\left(\theta_{j-1}\right)^4.\left[h^2 + (1/4).R_{j-1}^2 + \left(h^2 + R_j^2.\sin\left(\theta_j\right)^2/\sin\left(\theta_{j-1}\right)^2\right)\right]$$

$$\Phi_4 = R_j^2.\sin\left(\theta_j\right)^4.\left[h^2 + (1/4).R_j^2 + \left(h^2/\sin\left(\theta_j\right)^2\right)\right] + (1/4).h^4$$

The relative simulation error of the spherical layer (g) is calculated by the equation (53):

$$\delta_{maud_g} = \left(\left|U_g^{ideal} - U_g^{maud}\right|/U_g^{maud}\right).100\% \quad (53)$$

As for the determination of the relative computational error $\delta_{deduction}$, the spherical layer (g), It is calculated from the equation (54):

$$\delta_{deduct_g} = \left(\left|U_g^{ideal} - U_g^{generl}\right|/U_g^{ideal}\right).100\% \quad (54)$$

The geometric method for calibration of spherical tanks is superior to the volumetric calibration methods in accuracy, which is considered the most accurate and reliable in the field of calibration of all types of tanks. In addition, the performance according to this method has increased relative to analogues of other methods from tanks of the same volume by 2.5-2.7 times. A similar approach can be applied to other types of tanks **[18]**.

k. Calibration technique for non-metric digital cameras using terrestrial laser scanners:

Terrestrial laser scanners can be used to determine calibration parameters for non-metric digital cameras. A digital camera is used to photograph a test object from several points in space. Calibration parameters for non-metric digital cameras (internal orientation elements, radial and diamond distortion, external orientation elements, lens aberrations), Figure (5) also shows the main stages of the calibration procedure for non-metric digital cameras using a ground-based laser scanner **[20]**.

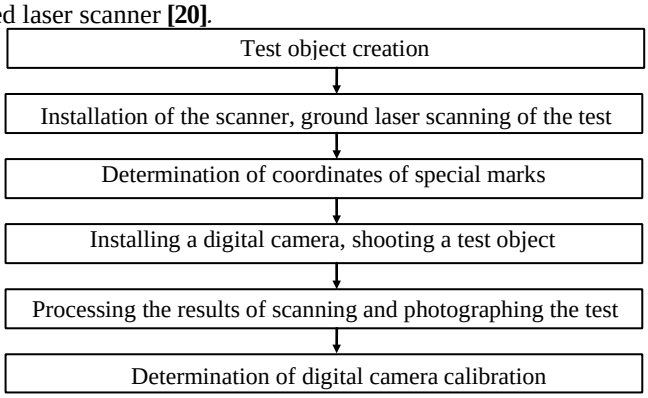

Figure.5. The main stages of calibration of digital non-metric cameras according to ground laser survey data [20].

To create a test object, special reflective marks are used, which are selected in accordance with the recommendations of the scanner manufacturer. it is necessary that they are scattered across the entire field of the picture. To ensure the relief of the test object in order to increase the reliability of the calibration results, you should set the following maximum S max and minimal S min the distance from the digital camera to the points of the test, [9] Using the equation (55):

$$(S_{max} - S_{min}/S) \geq \frac{1}{3} \quad (55)$$

Where:

S: the average distance to the points of the test object.

In theory, the accuracy of determining the coordinates of the marking centers is higher if the scanner is as close to the marks as possible. In addition, the results of the scanner calibration showed that the highest accuracy in determining the coordinates of the special marking centers by different scanners is achieved at different distances. Therefore, for each scanner model, the optimum marker distance must be determined from experimental studies. It follows that the laser scanner must be positioned symmetrically relative to the points of the test object and approximately at the same distance from them in order to exclude the influence of changes in the distance between the marks from the scanner on the accuracy of determining the coordinates of the points of the test object. When photographing a test object with a non-metric digital camera Before shooting, it is necessary to justify the number of shooting stations and their location, which shoot the entire test object with a minimum number of photographic points and ensure the specified accuracy of camera calibration. the accuracy of systematically identifying distortions in the plane coordinates of the digital image points increases in proportion to the square root of the ratio $(t + 1)\ t^2$ (t: number pictures). Therefore, we can conclude that the practical stability of the calibration results is observed when the number of images is from 15 to 20. This number of images can be taken as sufficient and optimal **[7]**.

When performing studies of a digital non-metric camera, it is proposed to shoot a test object from four photographs points, while four to five photographs should point. To determine the coordinates of the points of the test object with a given accuracy, it is necessary to set the distance between the camera and the object, calculated by the equation (56) **[20]**:

$$S = (3\delta x f/mx) \quad (56)$$

Where:

mx: the mean square error in determining the coordinates of test points.

δx: error in determining the coordinates of point of the test object using the scanner.

f: focal length of the camera.

To determination of camera calibration parameters and exterior orientation elements of images. After the end of the ground laser scanning and photographing of the test object, the following works are performed **[17]**:

1. processing of data obtained by a ground-based laser scanner in order to determine the spatial coordinates of points of the test object (special marks).
2. measurement of coordinates of images of centers of special marks on digital images.
3. calculation of camera calibration parameters.

4. assessment of the accuracy of determining the calibration parameters and preparation of couple.

To calibrate cameras using images of a special test object, collinear conditions are used. As functions for describing systematic errors σx, σy, which are widely used to calibrate digital non-metric cameras, Using the equation (57):

$$\delta x = k_1 x r^2 + k_2 x r^4 + k_3 x r^6 + k_4 x r^8 + p_1(2x^2 + r^2) + 2p_2 xy$$
$$\delta y = k_1 y r^2 + k_2 y r^4 + k_3 y r^6 + k_4 y r^8 + p_2(2y^2 + r^2) + 2p_1 xy \quad (57)$$

Where:

k,p: coefficients describing the influence of radial and tangential distortion;

r: radius vector characterizing the position of the point on the image. By equation (58):

$$r = \sqrt{x^2 + y^2} \quad (58)$$

Where:

$$x = x - x_0$$
$$y = y - y_0$$

Evaluation of the accuracy of determining the calibration parameters. After determining the elements of external and internal orientation of images and coefficients of polynomials. Then, the residuals Δ x, Δ y, with the help of which the mean square errors are determined, which characterize the accuracy of image calibration, according to the equation (59) **[7]**:

$$m_{x_{caliber}} = \sqrt{\left(\sum_{i=1}^{n} \Delta x_i^2 / n\right)}$$
$$m_{y_{caliber}} = \sqrt{\left(\sum_{i=1}^{n} \Delta y_i^2 / n\right)} \quad (59)$$

Where:

n: the number of special stamps, the coordinates of which are measured on picture.

Practical work showed the following **[20]**:

1. Full digital camera calibration can be performed using a terrestrial laser scanner.
2. The accuracy of determining the coordinates of special marks by the scanner meets the requirements for creating test objects for calibrating cameras.
3. From the images of special marks located, a reliable determination of the camera calibration parameters is provided. **[21]**:

The main advantages of calibrating digital non-metric cameras using terrestrial laser scanners are:

1. Full automation of the calibration process, since special marks for all terrestrial laser scanners are made in such a way that they can be easily identified both on a digital image and on a point, model obtained as a result of scanning.
2. Eliminates the need to fix the points of the test object and create various kinds of structures.
3. Cameras can be calibrated both on a special test site and at the time of the very shooting of the object, since in the technology of ground laser scanning, special brands are used to combine scans obtained from several scanning stations into a single point model.

III. CONCLUSION

The research aims to solve some problems of laser scanning technology to meet the requirements of different fields of work. The main results of the research are summarized as follows: Clarifying the mathematical model of laser scanning technology during data collection, conducting a study of the general principles of measurement and processing operations, and taking into account the factors affecting the accuracy of these operations to obtain three dimensional models in an ideal way, on the basis of the proposed theory. Studies are conducted on individual sources of errors. And the formulation of the basic equation for the process of measuring angles and distances by ground-based laser scanners. Knowing the ideal geometric location and number of stamps to support the scanning process, and expanding the application of ground-based laser scanning technology, which leads to reducing the time required to establish a test range for calibrating a non-metric digital camera. Using the laser scanner to determine the sizes of spheroids based on the creation of a 3D model of their internal space according to ground-based laser scanning data. By developing an algorithm and software to evaluate the accuracy of calibration tanks using mathematical methods, and using the proposed method to determine the sizes of spheres allows reducing the relative error in determining the capacity to 0.03-0.05%, i.e. 2-3 times more accurate than previous calibration methods used.

The prospect of further development of the topic is related to the development of methods for automated compression and processing of laser scanning data based on the proposed theory of photogrammetric processing of laser scanning data. Optimization of the scanner hardware based on the proposed equation for the measurement process in order to improve the accuracy.

Funding: This research has not been conducted under any fund.

Conflicts of Interest: The authors declare that there is no conflict of interest.

REFERENCES

[1] Lemmens M, Lemmens M. Terrestrial laser scanning. Geo-information: technologies, applications and the environment. 2011:101-21.
[2] Mosalam KM, Takhirov SM, Park S. Applications of laser scanning to structures in laboratory tests and field surveys. Structural Control and Health Monitoring. 2014 Jan;21(1):115-34.
[3] Lichti DD. Ground-based laser scanners: operation, systems and applications. Geomatica. 2002 Jan;56(1):21-33.
[4] Ebrahim MA. 3D laser scanners' techniques overview. Int J Sci Res. 2015 Oct;4(10):323-31
[5 Newnham G, Armston J, Muir J, Goodwin N, Tindall D, Culvenor D, Püschel P, Nyström M, Johansen K. Evaluation of terrestrial laser scanners for measuring vegetation structure. Australia: CSIRO. 2012 Jun 4.
[6] Leader JC. Analysis and prediction of laser scattering from rough-surface materials. JOSA. 1979 Apr 1;69(4):610-28.

[7] Zhang Y, Shen X. Quantitative analysis on geometric size of LiDAR footprint. IEEE Geoscience and Remote Sensing Letters. 2013 Aug 26;11(3):701-5.
[8] Idrees MO, Pradhan B. A decade of modern cave surveying with terrestrial laser scanning: A review of sensors, method and application development. International Journal of Speleology. 2016.
[9] Jaafar HA, Meng X, Sowter A. Terrestrial laser scanner error quantification for the purpose of monitoring. Survey Review. 2018 May 4;50(360):232-48.
[10] Lichti DD, Licht MG. Experiences with terrestrial laser scanner modelling and accuracy assessment. Int. Arch. Photogramm. Remote Sens. Spat. Inf. Sci. 2006 Sep 25;36(5):155-60.
[11] Gardzińska A. Application of Terrestrial Laser Scanning for the Inventory of Historical Buildings on the Example of Measuring the Elevations of the Buildings in the Old Market Square in Jarosław. Civil and Environmental Engineering Reports. 2021 Jun;31(2):293-309.
[12] Barbarella M, Fiani M. Monitoring of large landslides by Terrestrial Laser Scanning techniques: field data collection and processing. European Journal of remote sensing. 2013 Jan 1;46(1):126-51.
[13] Park HS, Lee HM, Adeli H, Lee I. A new approach for health monitoring of structures: terrestrial laser scanning. Computer-Aided Civil and Infrastructure Engineering. 2007 Jan;22(1):19-30.
[14] Anton H, Rorres C. Elementary linear algebra: applications version. John Wiley & Sons; 2013 Nov 4
[15] Arayici Y. An approach for real world data modelling with the 3D terrestrial laser scanner for built environment. Automation in construction. 2007 Sep 1;16(6):816-29
[16] Liang H, Li W, Lai S, Zhu L, Jiang W, Zhang Q. The integration of terrestrial laser scanning and terrestrial and unmanned aerial vehicle digital photogrammetry for the documentation of Chinese classical gardens–A case study of Huanxiu Shanzhuang, Suzhou, China. Journal of Cultural Heritage. 2018 Sep 1; 33:222-30
[17] Moussa W. Integration of digital photogrammetry and terrestrial laser scanning for cultural heritage data recording
[18] Jiashun H, Xiaoxiao H. Applications of 3D Laser Scanning for Storage Tank: Review, Challenges and Outlook. In2017 Far East NDT New Technology & Application Forum (FENDT) 2017 Jun 22 (pp. 86-90).
[19] Mulholland GW, Bryner N, Liggett W, Scheer BW, Goodall RK. Selection of calibration particles for scanning surface inspection systems. InFlatness, Roughness, and Discrete Defect Characterization for Computer Disks, Wafers, and Flat Panel Displays 1996 Nov 4 (Vol. 2862, pp. 104-118). SPIE
[20] Lerma JL, Navarro S, Cabrelles M, Villaverde V. Terrestrial laser scanning and close-range photogrammetry for 3D archaeological documentation: the Upper Palaeolithic Cave of Parpalló as a case study. Journal of Archaeological Science. 2010 Mar 1;37(3):499-507
[21] Daneshmand M, Helmi A, Avots E, Noroozi F, Alisinanoglu F, Arslan HS, Gorbova J, Haamer RE, Ozcinar C, Anbarjafari G. 3d scanning: A comprehensive survey. arXiv preprint arXiv:1801.08863. 2018 Jan 24.